RSC Advances

PAPER

View Article Online
View Journal | View Issue

Cite this: *RSC Adv.*, 2015, **5**, 38503

Kinetic exploration supplemented by spectroscopic and molecular docking analysis in search of the optimal conditions for effective degradation of malachite green†

Somnath Dasmandal,[a] Harasit Kumar Mandal,[a] Suparna Rudra,[a] Arjama Kundu,[a] Tapas Majumdar[b] and Ambikesh Mahapatra*[a]

The degradation of malachite green (MG) by an alkaline hydrolytic process has been explored spectrophotometrically. The kinetics of the reaction have been meticulously studied under the influence of cationic alkyltrimethylammonium bromide (DTAB, TTAB and CTAB) surfactants, α-, β- and γ-cyclodextrins (CDs) and surfactant–β-CD mixed systems applying pseudo-first order conditions at 298 K. The surfactants and cyclodextrins individually catalyze the hydrolytic rate, whereas surfactant–β-CD mixed systems exhibit both an inhibiting and catalytic influence depending on the surfactant concentrations. The kinetic results have been explained precisely based on the pseudo-phase ion exchange (PIE) model of micelles and CD-catalyzed model of CD systems. The surfactants exhibit micellar surface catalysis, while CDs accelerate the rate by forming MG–CD inclusion complexes, thereby facilitating nucleophilic attack of its ionized secondary hydroxyl group on the carbocation center of MG. The encapsulation of MG within the supramolecular host cavity of the CDs has been investigated diligently using a steady-state absorption spectroscopic technique. The result shows 1 : 1 host–guest complexation with different relative orientations of the guest (MG) inside the hosts. Studies employing density functional theory (DFT) as well as molecular docking analysis provide valuable insight on the insertion mechanism. The results reveal that quantitative analysis can be utilized to predict the optimum conditions for the fastest degradation of MG in ambient environments.

Received 17th March 2015
Accepted 8th April 2015

DOI: 10.1039/c5ra04724b

www.rsc.org/advances

1. Introduction

The chemistry of dyes and their application in various scientific fields have attracted immense attention in modern times. Malachite green (MG) is an important dye of commercial and analytical importance.[1] However, the high solubility of the dye in water makes it a potential water pollutant. Contamination of water-systems by the dye creates a severe risk to aquatic living organisms through bioaccumulation and thus by entering the food chain. Thus the removal of the dye from industrial effluents in an economic fashion is a leading challenge. A number of methods have recently been used for dealing with the treatment of wastewater discharged from textile industries *viz.*, physico-chemical treatment by biological oxidation, adsorption and advanced oxidation processes (AOPs), *e.g.*, ozonation, photolysis, electrochemical, sonolysis *etc.*[2,3] Sometimes, these processes have been found to release more toxic products than the parent compound that prove fatal for the living creatures.[4] Hydrolysis is one of the prime detoxification mechanisms for organic compounds as the hydrolysis by-products are normally less toxic to the environment than the parent compound.[5] Thus in our present study we have extensively studied the kinetics of alkaline hydrolysis of malachite green in different micro-heterogeneous environments made up of surfactants, cyclodextrins and their mixed systems.

Microenvironments consisting of surfactants are capable of both catalyzing and inhibiting the hydrolysis rates depending on specific interactions between the surfactants and reactant species, micellar aggregation number, CMC values, the extent of incorporation of reactants as counter ions in micelles *etc.*[6,7] Not only surfactants, but also cyclodextrins, by virtue of their cage like structure, may influence the rate of hydrolysis reactions.[8] Cyclodextrins (CDs) are cyclic oligomers of α-D-glucose linked by α-1,4 glycoside bonds. Natural cyclodextrins are classified as α-, β- or γ-CD according to whether they have 6, 7 or 8 α-D-glucopyranose residues respectively.[9] CDs can form inclusion complexes by means of non-covalent interactions, including van der Waals, hydrophobic, electrostatic, hydrogen bonding,

[a]*Department of Chemistry, Jadavpur University, Kolkata 700 032, India. E-mail: amahapatra@chemistry.jdvu.ac.in; ambikeshju@gmail.com; Fax: +91 33 2414 6223; Tel: +91 33 2457 2770; +91 33 2432 4586*

[b]*Department of Chemistry, University of Kalyani, Kalyani 741 235, India*

† Electronic supplementary information (ESI) available. See DOI: 10.1039/c5ra04724b

steric effects *etc.* with molecules that fit into their cavities.[10,11] Because of their ability to form inclusion complexes, the reaction rates are generally reduced, *i.e.* CDs act here as stabilizers,[12] but more interest has been placed in the situation where CDs accelerate the reactions.[13] Moreover, surfactant–CD mixed systems have drawn great interest in recent years due to their numerous applications in commercial formulations.[14] These systems can be used as a model for establishing the effect of cyclodextrins on phospholipids, an essential part of cell membranes. The addition of cyclodextrin to a micellar solution alters its physicochemical properties.[15] This is due the formation of CD–surfactant inclusion complexes where the stoichiometries (CD : surfactant) for the majority of such cases are found to be 1 : 1 or 1 : 2 or even 2 : 1 depending on the type of surfactant, tail chain length and also the size of the CD cavity.[16]

A number of studies have already been reported separately on the basic hydrolysis of triphenylmethane dyes in the presence of cationic,[17] anionic[18] and non-ionic[19] surfactants, cyclodextrins[20] and their mixed systems.[21] Nevertheless, only little attention has been paid so far to determine the optimal operating environment for the efficient removal of dyes from wastewater using a hydrolysis process. According to the literature, anionic surfactants greatly retard the rate of alkaline hydrolysis reaction of triphenylmethane dyes.[18] On the contrary, cationic surfactants generally accelerate the rate and their accelerating effect is much pronounced than for the non-ionic surfactants.[19] Thus in our present study, we have used three cationic surfactants (DTAB, TTAB, CTAB) of different chain lengths to monitor their effect on the hydrolysis rate. Again, in the presence of CDs, the probable mechanistic pathway of their interaction with MG in an alkaline medium and their efficiency to degrade the dye are not yet known. Thus three CDs (α-, β-, γ-) of different cavity size have been used herein due to their ability to interact with MG and thereby influence the reaction rate. Besides, the insertion mechanism of MG inside the CD nanocavity has been carefully studied employing a steady-state absorption technique and molecular docking analysis to gain a better understanding of the experimental findings. Thus, the present study may help to find a system with an optimally balanced combination of surfactant and CD to degrade malachite green at a much faster rate. The reaction of malachite green in the presence of an alkali is a one-step reaction[22] and follows pseudo-first order kinetics. All the experimental results are discussed with proper correlation to the literature reports.

2. Materials and methods

2.1. Materials

Malachite green (MG) has been procured from Merck, India as a chloride salt, $[C_6H_5C(C_6H_4N(CH_3)_2)_2]Cl$ and used as received. The surfactants dodecyltrimethylammonium bromide (DTAB), tetradecyltrimethylammonium bromide (TTAB), cetyltrimethylammonium bromide (CTAB) or in general alkyltrimethylammonium bromide (ATAB) as well as α, β and γ-cyclodextrins (CDs) have been purchased in the highest available purity from TCI, Japan. All other organic solvents used in this study have been obtained from Merck, India. Highly purified water from Milli-Q Ultra has been used for all sample preparation and dilution.

2.2. Methods

2.2.1. Experimental. A fresh solution of malachite green (MG) was usually prepared for day to day work and used only after checking its concentration using the molar extinction coefficient, ε_{616} (MG) = 1.48×10^5 M^{-1} cm^{-1}.[23] The absorption spectra and kinetic measurements were recorded using a Shimadzu, UV-1800 Spectrophotometer equipped with a Peltier temperature controller, TCC-240A, maintaining a constant temperature of 298 K (±0.1 K). The kinetics of the alkaline hydrolysis were followed by measuring the decay in the absorbance at 616 nm as a function of time. A representative spectral change for the hydrolysis reaction is shown in Fig. S1†. The hydrolysis process has been investigated under pseudo-first order reaction conditions using NaOH in large excess. The hydrolysis of MG was usually followed up to 7–8 half-lives. In all the kinetic runs, the final concentration of MG was kept at 1.25×10^{-5} M and the ionic strength (μ) of the medium was maintained at 5.0 mM by adding KNO_3 solution. The observed first order rate constants (k_{obs}) and their standard deviations were obtained by fitting to the first order exponential decay of absorbance (A_t) *versus* time (t) plot using Microcal Origin 8.0.

2.2.2. Theoretical methodology. The crystal structures of α-, β- and γ-CDs were obtained from protein complexes (pdb id: 2ZYM, 2Y4S and 2ZYK for α-, β- and γ-CD respectively) available from the Protein Data Bank (PDB). The CDs were then extracted and all the hydrogen and Gasteiger charges added to prepare them for docking. The ground state geometry of malachite green (MG) was optimized employing density functional theory (DFT) in conjugation with B3LYP functional and 6-31G* basis set in Gaussian 09 program suit.[24] The PDB structure of MG was derived from the optimized structure. MG was considered as a ligand and CD as a receptor for docking studies. The molecular docking was carried out applying the Lamarckian Genetic Algorithm (LGA), inculcated in the docking program Auto Dock 4.2.[25] The CDs were laid over a three dimensional grid box ($126 \times 126 \times 126$) $Å^3$ with 0.375 Å spacing. The output from Auto Dock was analyzed using PyMOL software.[26]

3. Results and discussion

3.1. Kinetic study

3.1.1. Hydrolysis of malachite green in aqueous medium. Hydrolysis causes the disruption of the extensive conjugation present in malachite green and thereby results in gradual diminution of the colour intensity. The hydrolysis reaction starts with the attack of the nucleophile, ^-OH, to the carbocation center and results in the formation of a neutral carbinol base. The well-known mechanism of the reaction in the aqueous phase[27] is shown in Scheme 1. The overall order of the reaction is found to be second *i.e.* first order in each of the reactant species, $[MG]_0$ and $[^-OH]_0$.

The observed rate law can be expressed by eqn (1)

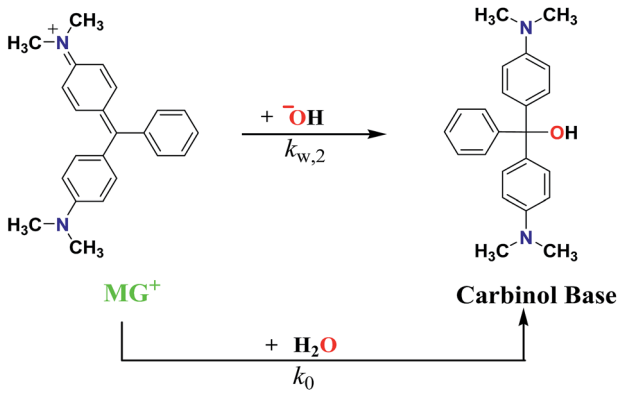

Scheme 1 Alkaline hydrolysis of malachite green (MG).

$$\text{Rate} = -\frac{d[MG]}{dt} = \{k_0 + k_{w,2}[^-OH]_0\}[MG]_0 \quad (1)$$

since, $[^-OH]_0 \gg [MG]_0$.

Therefore,

$$-\frac{d[MG]}{dt} = k_{obs}[MG]_0$$

where,

$$k_{obs} = k_0 + k_{w,2}[^-OH]_0 \quad (2)$$

where, $k_{w,2}$ is the second-order rate constant for the alkaline hydrolysis reaction. The value of $k_{w,2}$ determined from the slope of the plot k_{obs} *versus* $[^-OH]_0$ (by eqn (2)) is 2.508 (±0.05) M^{-1} s^{-1}. The rate constant for hydrolysis of MG in pure water (k_0) obtained from the intercept of the plot is found to be of 9.75 × 10^{-5} s^{-1}.

3.1.2. Hydrolysis of malachite green in micellar media. The influence of concentration of cationic amphiphiles (ATABs) on the rate of alkaline hydrolysis of malachite green (MG) has been examined over a wide interval that includes both the region prior to the CMC and the region after the CMC. (Fig. 1). Fig. 1 shows that k_{obs} increases only slightly on increasing the surfactant concentration until the CMC. This is an indication of weak pre micellar activity.[19] But afterwards, a sharp increase in k_{obs} can be observed due to the presence of micellar aggregates, and reaches a limiting value, beyond which k_{obs} starts to decrease considerably. The CMC values have been obtained kinetically as the minimum surfactant concentration required to induce a substantial change in the observed rate constant and found to be 11.3, 1.5 and 0.5 mM for DTAB, TTAB and CTAB respectively. These data show fair agreement with the literature values.[28] However, the CMCs derived kinetically are found to be lower than those shown by micellar systems of pure surfactants. This reduction has been ascribed to the known effect of electrolyte on CMC.

The alkaline hydrolysis of MG in cationic micellar media experiences micellar surface catalysis. An increment of surfactant concentration beyond its CMC leads to an increase in the number of the micelles in the bulk phase,[29] which in turn increases the concentration of micelle bound MG and ^-OH in the micellar Stern region. The MG is believed to be incorporated into the micelles by a hydrophobic interaction due to the existence of the phenyl moieties and ^-OH is gathered by a coulombic attraction effect. This observation is in accordance with our earlier findings.[30] However, the phenomenon of ion-exchange at the micellar interface plays a vital role in determining the limiting value of k_{obs}. The gradual addition of surfactant results in increasing the concentration of counterion, Br^- in the medium. These are nonreactive counterions. Hence, a competition between Br^- and ^-OH in the Stern region eventually inhibits the reaction rate.[31]

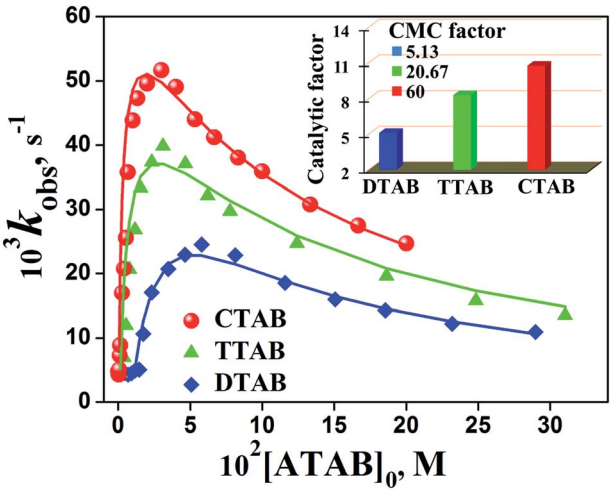

Fig. 1 Plots of k_{obs} *versus* concentration of surfactants with different chain lengths for alkaline hydrolysis of MG at 298 K. $[MG]_0 = 1.25 \times 10^{-5}$ M, $[^-OH]_0 = 1.875$ mM. Inset: catalytic factor (k_{obs}^{max}/k_w) in different micellar systems.

The experimental results can be interpreted quantitatively on the basis of the Pseudo-phase Ion Exchange (PIE) model.[32] This model uses the micellar pseudo-phase formalism (Scheme 2) coupled with the assumption of ion-exchange at the ionic micellar surface[33] and yields eqn (3).

$$k_{obs} = \frac{k_{w,2}[^-OH]_T + (K_{MG}^m k_m - k_{w,2})m_{OH}[D_n]}{1 + K_{MG}^m[D_n]} \quad (3)$$

where $k_{w,2}$ & k_m are the rate constants in aqueous and micellar pseudo-phases respectively. K_{MG}^m is the association constant between MG and the micelles. D_n represents the micellized surfactant ($[D_n] = [ATAB]_T - CMC$). m_{OH} is the $[^-OH]_m/[D_n]$ ratio, where ^-OH_m is the hydroxyl ion at the micellar surface.

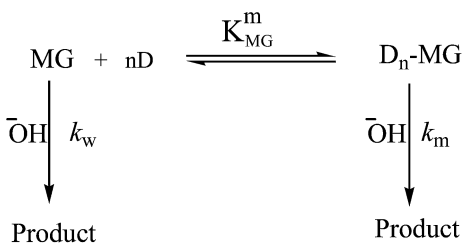

Scheme 2 Hydrolysis of MG in micellar solution.

The values of m_{OH} at different $[D_n]$ and at a constant $[^-OH]_T$ have been calculated by eqn (4)

$$m_{OH}^2 + m_{OH}\left[\frac{[^-OH]_T + K_{Br}^{OH}[Br^-]_T}{(K_{Br}^{OH}-1)[D_n]} - \beta\right] - \frac{\beta[^-OH]_T}{(K_{Br}^{OH}-1)[D_n]} = 0 \quad (4)$$

where β is the fraction of surfactant head groups neutralised by counterions ($\beta = 0.8$).[34] In order to resolve eqn (4), a value of $K_{Br}^{OH} = 15$ has been used as it gives the best fit of the theoretical line. Moreover, the value of K_{Br}^{OH} for the most widely studied systems containing hydroxide ion and bromide ion micelles fall within the range of 10–20.[35] The calculated values of m_{OH} are then used in eqn (3) to evaluate k_m, K_{MG}^m and least squares, $\sum d_i^2$ (where, $d_i = k_{obs,i} - k_{cal,i}$ with $k_{obs,i}$ and $k_{cal,i}$ representing the observed and calculated rate constant values at the i^{th} concentration of micellized surfactant, $[D_n]_i$) values using the non-linear least-squares technique. The value of k_w (first-order rate constant in the aqueous phase) is kept constant and identical to the value previously obtained in the aqueous phase. The values of k_m and K_{MG}^m so obtained from eqn (3) for different micellar systems are presented in Table 1 along with the calculated values of the rate constants, k_{cal}, at $K_{Br}^{OH} = 15$. A satisfactory fit of observed data to eqn (3) is evident from the plot of Fig. 1, where a solid line has been drawn by the calculated data points (k_{cal}) for different micellar systems employing the value of $K_{Br}^{OH} = 15$.

The lower values of K_{MG}^m for CTAB micelles compared to DTAB may be attributed to the fact that the longer hydrocarbon chain of CTAB may result in folding and thus provide less space for binding to MG.[36] Hence, the highest value of k_m in a CTAB micellar medium (Table 1) helps us to recognize the concurrent effect on the hydrolysis reaction caused by the increment of local concentration of the reactant species at the micellar surfaces and the lowering of polarity at the micellar pseudo-phase compared to the bulk aqueous phase.[19] The effect of polarity on the hydrolysis rate is well understood by the Hughes and Ingold rule: that is, the rate of the formation of a neutral product from two oppositely charged reactants gets accelerated as the polarity of the medium decreases.[37] The rate acceleration caused by lowering of polarity in the micellar Stern region has been discussed in our previous work too.[30] Moreover, CTAB being the highest homologue among the ATABs possesses the lowest value of CMC. Therefore, the concentration of the nonreactive counterion, Br^- in equilibrium with the CTAB micellar system is also much less when the micellization process begins. Thus, CTAB shows the maximum catalytic effect on the hydrolysis rate among the ATABs.

The characteristic behaviour of catalysis exhibited by all the cationic micelles (Fig. 1) allows us to compare quantitatively the catalytic influence of the surfactants on the rate of alkaline hydrolysis of malachite green. The catalytic effect is found to increase towards the higher homologues of ATABs *i.e.*, it follows the order: DTAB ($-C_{12}$) < TTAB ($-C_{14}$) < CTAB ($-C_{16}$). The maximum degree of catalytic activity in different micellar systems is shown in the Fig. 1 inset introducing the parameter, catalytic factor (k_{obs}^{max}/k_w), and for each value of k_{obs}^{max}/k_w, the corresponding concentration of surfactant has been presented in terms of CMC factor ([ATAB] for k_{obs}^{max} to CMC ratios). As can be seen from Fig. 1 & inset, the catalytic effect exerted by the CTAB micellar system reaches a maximum degree at [CTAB] of 30.0 mM which is nearly 60 times its CMC under the conditions of our present study. While TTAB and DTAB exhibit their maximum catalytic activity at concentrations corresponding to 20 times and 5 times to their respective CMC values.

Table 1 Kinetic parameters for alkaline hydrolysis of MG in presence of surfactants at 298 K[a]

DTAB			TTAB			CTAB		
$10^3[DTAB]_0$, M	10^3k_{obs}, s^{-1}	10^3k_{cal},[b] s^{-1}	$10^3[TTAB]_0$, M	10^3k_{obs}, s^{-1}	10^3k_{cal}, s^{-1}	$10^3[CTAB]_0$, M	10^3k_{obs}, s^{-1}	10^3k_{cal}, s^{-1}
0.0	4.80	—	0.0	4.81	—	0.0	4.80	—
11.6	4.89 ± 0.1[c]	5.20	1.6	4.44 ± 0.1	5.11	0.67	5.1 ± 0.1	8.81
14.5	5.07 ± 0.1	9.43	3.9	6.95 ± 0.1	18.13	1.00	7.3 ± 0.1	14.99
17.4	10.66 ± 0.2	12.69	7.8	20.64 ± 0.3	28.06	2.67	17.0 ± 0.2	31.48
23.2	17.07 ± 0.3	17.19	11.7	26.84 ± 0.2	32.72	4.0	20.8 ± 0.4	37.92
34.8	20.72 ± 0.3	21.50	15.5	33.29 ± 0.5	35.13	6.67	35.8 ± 0.8	44.79
46.4	22.93 ± 0.5	22.81	23.3	37.33 ± 0.7	36.99	10.0	43.9 ± 1.1	48.67
58.0	24.52 ± 0.3	22.83	31.1	39.84 ± 0.6	37.11	20.0	49.6 ± 1.3	51.09
81.2	22.86 ± 0.6	21.48	46.6	37.10 ± 0.4	35.61	30.0	51.7 ± 0.8	49.76
116.0	18.56 ± 0.5	18.82	77.6	29.73 ± 0.3	31.34	40.0	49.1 ± 1.0	47.61
150.8	15.99 ± 0.4	16.45	124.2	24.71 ± 0.4	25.88	66.7	41.2 ± 0.7	41.64
185.6	14.31 ± 0.1	14.53	186.3	19.62 ± 0.2	20.81	100.0	35.9 ± 0.8	35.54
232.0	12.23 ± 0.2	12.52	248.4	15.81 ± 0.2	17.35	133.3	30.8 ± 0.9	30.88
290.0	10.92 ± 0.3	10.65	310.5	13.49 ± 0.1	14.86	200.0	24.7 ± 0.5	24.39
$10^6\sum d_i^2$		0.098			0.447			13.849
k_m, s^{-1}		9.7 ± 0.5			15.1 ± 0.6			18.3 ± 0.9
K_{MG}^m, M^{-1}		21.5 ± 0.3			9.1 ± 0.4			9.3 ± 0.4

[a] $[^-OH]_0 = 1.875$ mM. [b] Calculated from eqn (3) and (4) with $\beta = 0.8$, $K_{Br}^{OH} = 15$, $k_{w,2} = 2.508$ M^{-1} s^{-1}. [c] Error limits are standard deviations.

3.1.3. Influence of α-, β- and γ-cyclodextrins on the reaction rate. The influence of cyclodextrins (CDs) on the rate of alkaline hydrolysis of MG is shown in Fig. 2. As can be observed, all the CDs catalyze the hydrolysis reaction, but to different extents. The maximum catalytic influence of the CDs is presented in the Fig. 2 inset in terms of catalytic factor (k_{obs}^{max}/k_w) at a common fixed CD concentration (1.0 mM). The experimental behaviour can be explained by taking into consideration the mechanistic behaviour as shown in Scheme 3 where CD-catalyzed and hydrolytic reaction take place through an MG–CD inclusion complex and in the bulk aqueous phase respectively. The catalytic effect exerted by CD can be attributed to the nucleophilic attack by the ionized secondary hydroxyl group of CD on the MG associated with CD.[38] Therefore, it must be assumed that the geometry of the inclusion complex formed by CDs of different cavity size is influential here for the rate variations found in Fig. 2.

In the presence of CD, binding of MG inside the host (CD) cavity gives the reaction an intramolecular character which enhances the rate of the reaction. This concept is quite similar to enzyme-like catalysis.[39] The supramolecular hosts bind MG in such a way that the electrophilic centre of the carbocationic dye is positioned close to the deprotonated secondary hydroxyl groups of CD. The proximity of the two groups in different MG–CD inclusion complexes will determine the efficiency of catalytic behaviour of the respective CDs.[40]

According to the Scheme 3, for a substrate that experiences an uncatalyzed reaction in a given medium as well as a catalyzed reaction by the formation of a 1 : 1 substrate–CD complex, the expected variation of k_{obs} with CD concentrations can be given by eqn (5).[38]

$$k_{obs} = \frac{k_w + k_{CD}K_{MG}^{CD}[CD]_0}{1 + K_{MG}^{CD}[CD]_0} \quad (5)$$

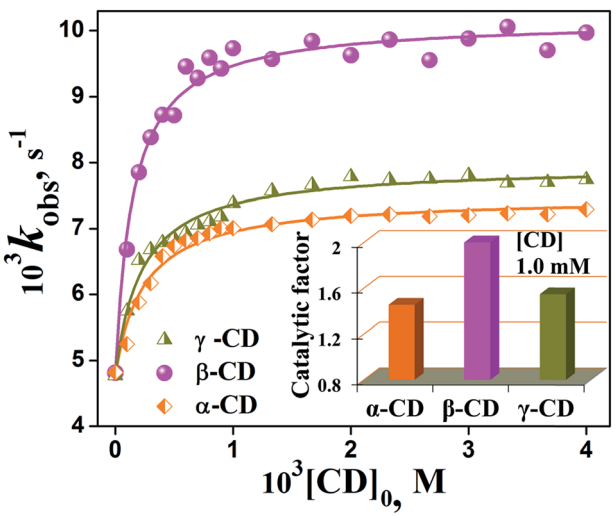

Fig. 2 Plots of k_{obs} *versus* $[CD]_0$ for the reaction of MG and ^-OH in aqueous medium at 298 K. $[MG]_0 = 1.25 \times 10^{-5}$ M, $[^-OH]_0 = 1.875$ mM. Inset: catalytic factor (k_{obs}^{max}/k_w) in different cyclodextrin systems at fixed [CD] = 1.0 mM.

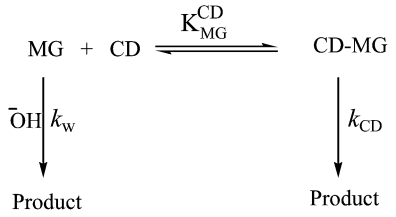

Scheme 3 Hydrolysis of MG in aqueous solution of CD.

K_{MG}^{CD} is the equilibrium binding constant of MG to the cyclodextrin, and k_{CD} is the pseudo-first order rate constant for the CD-catalyzed reaction. The value of k_w is kept constant and identical to the value previously obtained in the aqueous phase. The K_{MG}^{CD} and k_{CD} values are obtained by fitting the experimental data to eqn (5) by a non-linear regression analysis and are presented in Table 2. The k_{CD} values indicate that the rate acceleration by CDs follows the order: β-CD > γ-CD > α-CD *i.e.*, β-CD catalyzes the reaction to the most extent among the CDs.

The mechanism of the CD-catalyzed process is shown in Scheme 4, where cyclodextrin as its oxyanion reacts with the carbocationic dye (MG) resulting in a tetrahedral complex. Thus we have to consider not only the closest approach of the two reacting centers, but also the geometric change of the MG–CD complex needed for the entire reaction for a suitable orientation of the tetrahedral complex so formed.[41] A detailed conformational search regarding different geometrical orientations of MG inside the various CD cavities have been undertaken in the following sections *viz.* 4.1 & 4.2 based on steady-state absorption and molecular docking studies respectively in order to ascertain the observed rate variation in different CD systems.

Thus, Table 1 clearly reveals that the alkaline hydrolysis reaction is catalyzed to the highest extent in the presence of CTAB micellar medium among the ATABs. Similarly, β-CD accelerates the reaction most efficiently among the CDs (Table 2). Therefore, a kinetic study of the influence of surfactant concentration on the hydrolysis reaction at a fixed [CD] would provide guidance to reach the optimal conditions for the fastest degradation of MG. In this context, only β-CD has been chosen as a component of the surfactant–CD mixed system because of its better catalytic activity than α- or γ-CD.

3.1.4. Influence of ATAB–β-CD mixed systems on the reaction rate. The influence of surfactant concentration on k_{obs} for alkaline hydrolysis of MG in the presence of a constant concentration of β-CD, $[\beta\text{-CD}]_0 = 1.0$ mM is shown in Fig. 3. As we increase the surfactant concentration, k_{obs} initially decreases until it reaches a minimum value. This fact is attributed to the complexation of surfactant monomer with β-CD displacing MG to the bulk phase. The CD catalytic route thereby is lost and consequent reduction of the rate is observed. Dorrego and coworkers reported a similar observation with the base hydrolysis of *m*-nitrophenylacetate in mixed systems made up of alkyltrimethylammonium micelles and α- or β-cyclodextrins.[28] After the minima of the curve k_{obs} *versus* [ATAB], k_{obs} exhibits the same kind of [ATAB] dependence as we have observed in the

Table 2 Kinetic parameters for alkaline hydrolysis of MG in the presence of CDs at 298 K[a]

	α-CD		β-CD		γ-CD	
$10^3[CD]_0$, M	10^3k_{obs}, s^{-1}	10^3k_{cal},[b] s^{-1}	10^3k_{obs}, s^{-1}	10^3k_{cal}, s^{-1}	10^3k_{obs}, s^{-1}	10^3k_{cal}, s^{-1}
0.0	4.82	4.80	4.81	4.80	4.77	4.80
0.20	5.88 ± 0.04[c]	5.96	7.85 ± 0.05	7.89	6.52 ± 0.08	6.29
0.40	6.58 ± 0.06	6.41	8.73 ± 0.10	8.73	6.79 ± 0.07	6.84
0.60	6.82 ± 0.02	6.64	9.46 ± 0.11	9.12	6.94 ± 0.09	7.12
0.80	6.93 ± 0.08	6.79	9.59 ± 0.08	9.35	7.11 ± 0.08	7.29
1.00	7.01 ± 0.04	6.89	9.73 ± 0.04	9.50	7.38 ± 0.08	7.40
1.33	7.07 ± 0.10	6.99	9.57 ± 0.07	9.66	7.57 ± 0.4	7.53
2.00	7.19 ± 0.05	7.11	9.62 ± 0.07	9.83	7.79 ± 0.05	7.67
2.33	7.22 ± 0.05	7.15	9.86 ± 0.04	9.87	7.74 ± 0.03	7.71
3.00	7.21 ± 0.3	7.20	9.88 ± 0.06	9.94	7.81 ± 0.7	7.77
3.33	7.23 ± 0.03	7.22	10.06 ± 0.03	9.97	7.69 ± 0.5	7.79
4.00	7.29 ± 0.04	7.25	9.97 ± 0.04	10.01	7.74 ± 0.04	7.83
$10^6\sum d_i^2$		0.308		0.652		0.244
10^3k_{CD}, s^{-1}		7.4 ± 0.10		10.3 ± 0.11		8.0 ± 0.08
K_{MG}^{CD}, M^{-1}		4050 ± 90		6700 ± 110		4370 ± 80

[a] $[^-OH]_0 = 1.875$ mM. [b] Calculated from eqn (5), $k_w = 4.8 \times 10^{-3}$ s^{-1}. [c] Error limits are standard deviations.

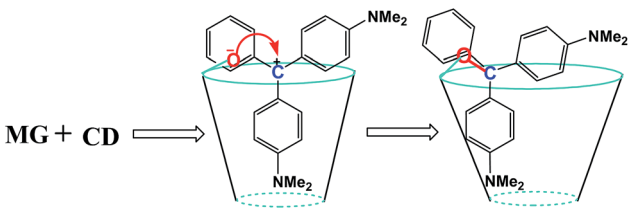

Scheme 4 Mechanism of hydrolysis reaction in CD medium.

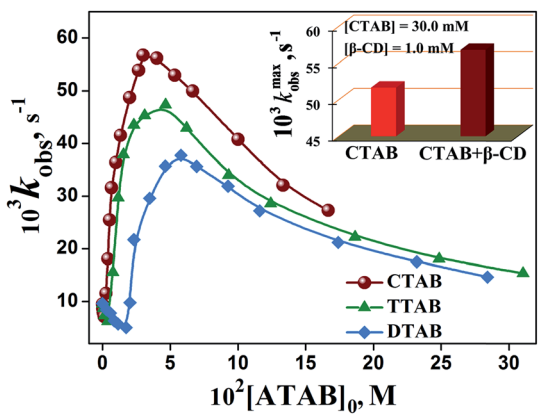

Fig. 3 Influence of ATAB concentration on k_{obs} for alkaline hydrolysis of MG in the presence of β-CD. $[β\text{-CD}]_0 = 1.0$ mM, $[^-OH]_0 = 1.875$ mM, $T = 298$ K. Inset: maximum rate constant, k_{obs}^{max}, in CTAB–β-CD mixed and CTAB micellar systems.

absence of CD, that is it increases rapidly up to a limiting value and falls gradually thereafter. The concentration of surfactant at that minimum value of k_{obs} has been taken as the onset of micellization and found to be 17.5, 3.6 and 1.5 mM for DTAB, TTAB and CTAB respectively. The CMCs have been found to be displaced to higher values than those of the respective surfactants in the absence of CD. This fact is ascribed solely to the complexation of surfactant monomers with β-CD.[16] At [ATAB] > CMC, the observed catalytic effect is due to the micellar catalysis by ATAB micelles and it is similar to what we have found in section 3.1.2. The catalytic efficiency of the mixed systems can be identified by the catalytic factor, *i.e.* the ratio of the observed rate constant at the maximum, k_{obs}^{max}, to that at micellization concentration, k_{obs}^{min}. The catalytic factor, $k_{obs}^{max}/k_{obs}^{min}$, of the various mixed systems has been found to be 7.5, 7.58 and 7.72 for DTAB, TTAB and CTAB respectively. The value of $k_{obs}^{max}/k_{obs}^{min}$ is quite independent on the nature of the surfactants. This result contrasts with the values of $k_{obs}^{max}/k_w = 5.11$, 8.51 and 11.39 for the same surfactants in pure micellar systems. This loss of catalytic efficiency of the surfactants in the mixed systems is due to the complexation between the surfactant monomer and β-CD. This is because the complexation displaces the CMC to higher values, which in turn increases the concentration of non-reactive counterions (Br^-) at the point of micellization. Moreover, the percentage of uncomplexed β-CD in equilibrium with the micellar systems increases together with the length of the hydrocarbon chain of the surfactants.[28] The increase in concentration of uncomplexed β-CD causes a shift in the minimums of the curves k_{obs} *versus* [ATAB] to a higher value of k_{obs} as the chain length of the surfactants increases. Both of the above incidents reduce the value of $k_{obs}^{max}/k_{obs}^{min}$.

As we are concerned about the fastest degradation of malachite green, that is the value of the maximum rate constant, k_{obs}^{max}, then it can undoubtedly be seen that the CTAB–β-CD mixed system is the most efficient environment in this scenario (Fig. 3 inset). Fig. 3 inset shows a comparison of the k_{obs}^{max} value between CTAB–β-CD mixed and CTAB micellar systems and it is observed that k_{obs}^{max} acquires a higher value in the CTAB–β-CD mixed system than in pure CTAB micellar system. Hence, the desired optimum conditions for the most effective degradation of malachite green is found to be $[CTAB]_0 = 30$ mM at $[β\text{-CD}]_0 = 1.0$ mM.

4. Characterization of MG–CD inclusion complex

4.1. Absorption studies

The change in absorption spectra of MG upon the quantitative addition of CD implies a significant interaction between them. Fig. S2† shows that the absorbance of MG at 616 nm decreases gradually with CD concentration. The stoichiometry of binding between MG and CDs has been ascertained using Benesi–Hildebrand (B–H) equation (eqn. (6)):[42]

$$\frac{1}{\Delta A} = \frac{1}{A' - A^0} + \frac{1}{K(A' - A^0)[\mathrm{CD}]_0} \quad (6)$$

where A^0 is the initial absorbance of the free guest (MG), ΔA is the change in absorbance of the inclusion complex (MG–CD), A' is the absorbance at the highest concentration of CD. The experimental results show a linear plot for $1/(\Delta A)$ *versus* $1/[\mathrm{CD}]_0$ throughout the entire concentration range for all the CDs. This clearly indicates 1 : 1 MG–CD complexation.[43] Fig. 4 shows the B–H plots for MG–β-CD, MG–α-CD and MG–γ-CD inclusion complexes. The association constant (K) of the host–guest inclusion complexes have been evaluated from the intercept and slope of these plots, and found as 4.89 (±0.07) × 10^2, 21.04 (±0.04) × 10^2 and 5.42 (±0.03) × 10^2 M^{-1} for α-CD, β-CD and γ-CD respectively.

The above results indicate that MG links to only one CD molecule. To substantiate the discussion, the molecular dimensions of MG have been calculated theoretically using the DFT method (Scheme 5) with B3LYP functional and 6-31G* basis set, and the data indicates that the complete incorporation of MG inside any of the CD cavities is not possible. It is well reported that CD molecules acquire a truncated, right-cylindrical, cone-shaped structure with a height of 7.8 Å and central cavities with diameters of the narrower and wider rim of α-, β- and γ-CD are 4.5–5.7 Å, 6.2–7.8 Å and 7.9–9.5 Å respectively.[44,45]

Keeping in mind the spatial distribution of the three phenyl rings and the size of MG (height and width), it is clear that only a part of MG can enter inside the CD cavity as shown in Scheme 5.

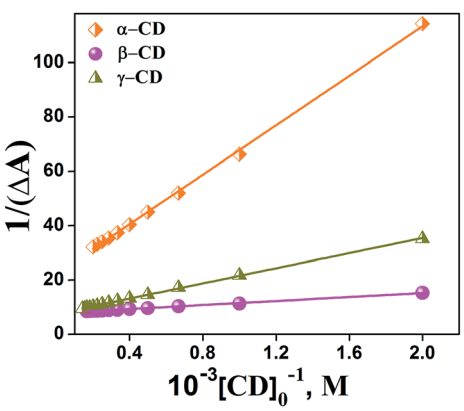

Fig. 4 Benesi–Hildebrand plot for the 1 : 1 MG–CD inclusion complexes in aqueous media.

The length of each of the phenyl rings bearing the –NMe_2 (dimethylaminobenzene) group (6.12 Å) and that of the benzene moiety (3.97 Å) of MG are compatible with the height of the CD cavity. Thus, during the process of inclusion, it is possible for the dimethylaminobenzene part of MG to penetrate the CD cavity, keeping the benzene moiety exposed to the bulk water, or *vice versa*. If MG orients in the latter pattern, there is no scope for change in the spectral behaviour, this is because in this situation the extended conjugated part of MG containing the auxochrome, –NMe_2, remains outside the CD cavity. Therefore, a considerable change in the absorption of MG can only be produced if the dimethylaminobenzene part is inside the CD cavity.

The minute change in the absorption profile of the MG–α-CD system indicates the weak interaction between α-CD and the dimethylaminobenzene moiety (6.12 Å). It is presumably due to the dimensional incongruity, thereby producing the small value, 4.89 (±0.07) × 10^2 M^{-1} of association constant (K) for MG–α-CD inclusion complex. However, the considerable diminution in absorbance of MG upon the quantitative addition of β-CD (up to 6 mM) is probably due to excellent dimensional compatibility between the dimethylaminobenzene moiety (6.12 Å) and the β-CD cavity (6.2–7.8 Å), indicating effective interaction between them (Scheme 5). This is reflected by the large value of K, 21.04 (±0.04) × 10^2 M^{-1} for the MG–β-CD inclusion complex. The significant change in the absorption profile of the MG–γ-CD system clearly supports the inclusion of the dimethylaminobenzene part inside the γ-CD core. But the much larger γ-CD cavity (7.9–9.5 Å) compels us to predict the two types of inclusion complexes, where the dimethylaminobenzene moiety (6.12 Å) may enter inside the γ-CD core either alone or together with the benzene moiety (3.97 Å). It is evident that both forms of the MG–γ-CD complex are capable of inducing a considerable change in the absorption behaviour of MG in γ-CD medium.

4.2. Molecular docking studies

Molecular docking is frequently used to predict the orientation of a guest molecule relative to a receptor when bound to each other.[46,47] Molecular docking analysis is accomplished herein to predict the probable location of MG within the complex architecture of cyclodextrins. The convergence of the conformational search employing the molecular docking model indicates the reliability of the experimental results for extracting structural orientations.

According to the docking model, the relative orientation of MG inside the α-CD nanocavity (Fig. 5a) allows us to identify a vertical mode of insertion of the benzene moiety with a binding energy of −5.38 kcal mol^{-1}. Another docked conformation (not shown) with dimethylaminobenzene as the inserting moiety (−2.7 kcal mol^{-1}) is also found to form. It is evident that the latter docked form is energetically less contributing to the MG–α-CD inclusion complex. Hence the minute change in the absorption behaviour of MG in α-CD medium is well justified by the latter docked form (Fig. S2a†). In β-CD, the dimethylaminobenzene moiety of MG inserts in a somewhat tilted fashion

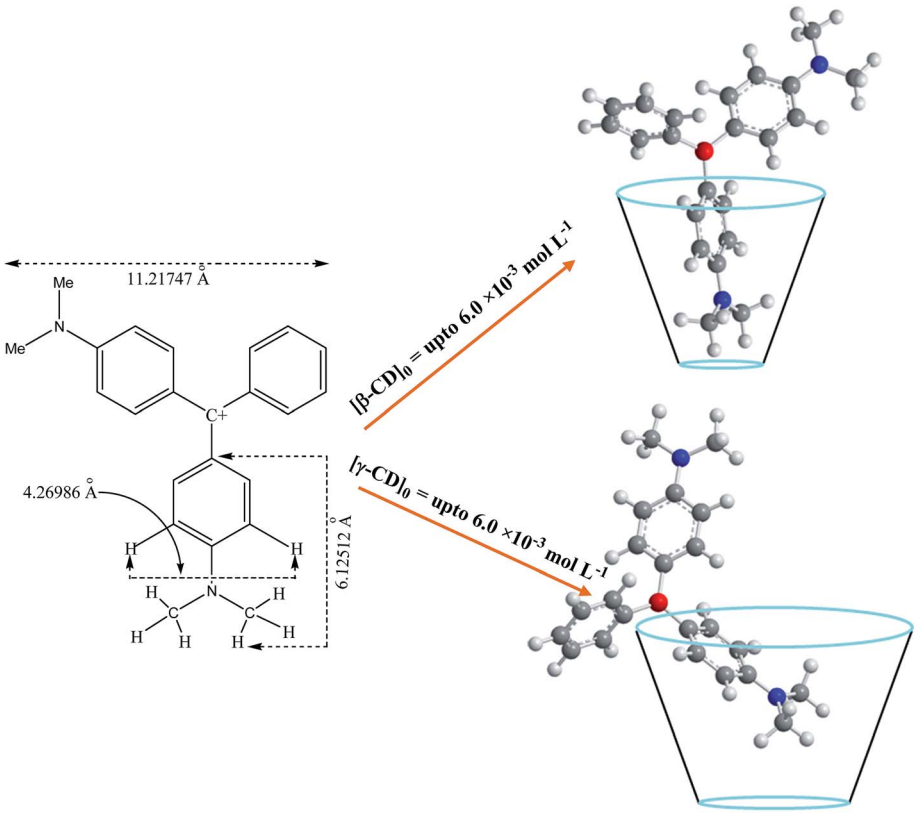

Scheme 5 Inclusion of MG inside the CD cavity.

producing a binding energy of −5.44 kcal mol^{-1} (Fig. 5b). The high negative binding energy with a torsional energy of 1.49 kcal mol^{-1} clearly reveals that MG snugly fits into the host cavity. The large diminution in absorbance of MG in the presence of β-CD fairly well supports the effective interaction between MG and β-CD (Fig. S2b†). However, the other docked form, albeit energetically less favourable (−4.98 kcal mol^{-1}), is also found to be formed by the benzene moiety as inserting group in the same

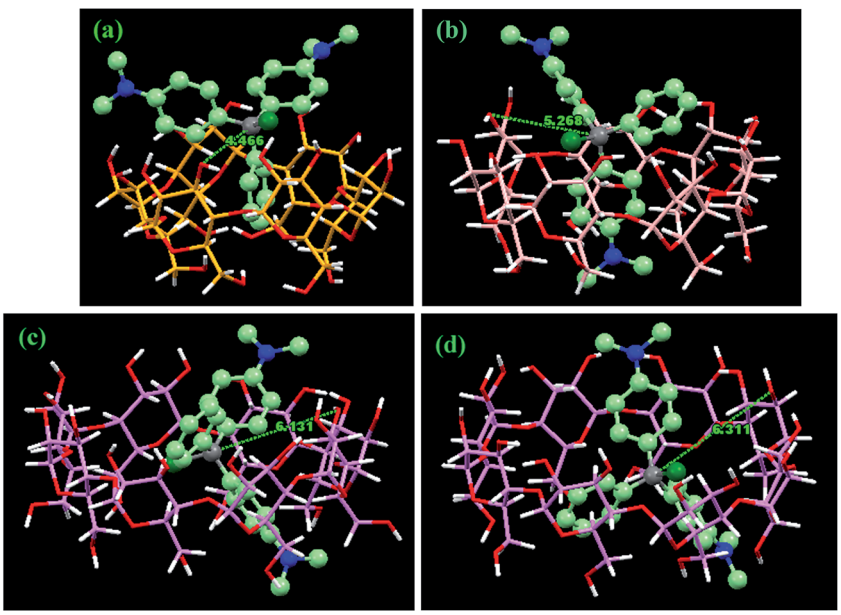

Fig. 5 Molecular docking of 1 : 1 complex for (a) MG–α-CD, (b) MG–β-CD, (c) MG–γ-CD (tilted) and (d) MG–γ-CD (horizontal). MG and CDs are depicted in the ball stick and capped stick model respectively (distances given in the pictures are in Å).

tilted fashion (Fig. S3†). In the case of γ-CD, the large cavity volume (7.9–9.5 Å) indeed strongly prohibits the benzene moiety (3.97 Å) inserting alone inside the host. The docked conformations in Fig. 5c and d show that MG orients itself in the two most probable arrangements inside the γ-CD core. One exhibits a bent vertical insertion of the dimethylaminobenzene moiety (Fig. 5c), and another shows the horizontal insertion of the same together with the benzene moiety (Fig. 5d) inside the empty pocket of the γ-CD. The considerable change in the absorption profile of the MG–γ-CD system is justified once again by the two docked forms (Fig. S2c†). Between the two docked forms, the latter has a binding energy of −5.79 kcal mol^{-1}, seems more favourable to be formed than the first one (−4.99 kcal mol^{-1}) with the same torsional energy (1.49 kcal mol^{-1}). As we have stated previously that the proximity of the attacking group (here, the deprotonated secondary hydroxyl group of CD) to the electrophilic center of the carbocationic dye plays a vital role over the rate variation in different CD environments. The distance between the carbocation center and the closest secondary hydroxyl is 5.268 Å in β-CD, but only 4.466 Å in α-CD (Fig. 5a and b). Therefore, nucleophilic attack by the ionized secondary hydroxyl group seems to be taking place with greater ease in the MG–α-CD inclusion complex. But the lower catalytic effect produced by α-CD (Table 2) makes us believe that the required geometric change of the product to a tetrahedral arrangement is difficult due to the small cavity size of α-CD and this fact outweighs the privilege acquired by the nearest approach of the two reacting centers. Whereas, in γ-CD, it is seen that the inserting groups of MG penetrate deeply inside the γ-CD core (Fig. 5c and d) producing a long distance between the two reacting centers (6.131 Å and 6.311 Å for Fig. 5c and d respectively). Therefore, the initial nucleophilic attack by the deprotonated secondary hydroxyl of γ-CD to the electrophilic center of the dye occurs only to a lesser extent. Hence, the order of catalytic effect of CDs that we found from kinetic studies (*i.e.*, β-CD > γ-CD > α-CD) is well justified by the above absorption and molecular docking studies.

5. Conclusion

Our target was to find the optimum conditions in terms of surfactant and CD concentration at ambient pressure and temperature to degrade MG proficiently by an alkaline hydrolysis process. In this context, among the C12, C14 and C16 variants of ATABs, the C16 homologue (CTAB) shows a marked catalytic effect on the hydrolytic rate. Similarly, among α-, β- and γ-CDs, β-CD having an appropriate cavity size exhibits effective interaction with MG and thereby facilitates appreciably the nucleophilic attack of its ionized secondary hydroxyl group to the carbocation center of MG. The rate variation by the CDs is manifested by the 1 : 1 host–guest inclusion complexes between MG and CDs. The relative orientations of MG inside the CD nanocavities are unveiled by the steady-state absorption technique along with quantum mechanical calculations using density functional theory (DFT) and molecular docking analysis. All of these studies indicate that the geometric fit of MG within different CD cavities will determine the efficiency of the catalytic activity of the respective CDs. A mixed system composed of CTAB and β-CD eventually provided the required results for this study exhibiting the maximum value of k_{obs} among all the ATAB–β-CD mixed systems. The conditions for the fastest degradation of MG by an alkaline hydrolysis process have been achieved at $[CTAB]_0 = 30$ mM in presence of $[\beta\text{-CD}]_0 = 1.0$ mM at normal temperature and pressure. Thus, the present study explicitly points towards an efficient route for the decontamination of malachite green from industrial wastewater in a comparatively greener way.

Acknowledgements

SD sincerely acknowledges University Grants Commission (UGC), New Delhi, for a junior research fellowship and AK acknowledges the Council of Scientific and Industrial Research (CSIR), New Delhi, for a senior research fellowship. TM gratefully acknowledges UGC, Govt. of India for funding with BSR-Startup grant (no. F.20-35/2013 (BSR) dated 09.12.2013) and UGC SAP program to Dept. of Chemistry, University of Kalyani.

References

1 D. F. Duxbury, *Chem. Rev.*, 1993, **93**, 381–433.
2 L. S. Andrade, L. A. M. Ruotolo, R. C. Rocha-Filho, N. Bocchi, S. R. Biaggio, J. Iniesta, V. Garčıa-Garcia and V. Montiel, *Chemosphere*, 2007, **66**, 2035–2043.
3 F. Robina, R. Faiza, B. Sofia, S. Maria, K. Sajjad, F. Umar, R. Abdur, F. Ather, P. Arshed, M. al Hassan and S. F. Shaukat, *World Appl. Sci. J.*, 2009, **6**, 234–237.
4 F. Robina, L. F. Kai, S. F. Shaukat and J. J. Huang, *J. Environ. Sci.*, 2003, **5**, 710–714.
5 W. R. Mabey and T. Mill, *J. Phys. Chem.*, 1978, **7**, 383–415.
6 A. S. Al-Ayed, M. S. Ali, H. A. Al-Lohedan, A. M. Al-Sulaim and Z. A. Issa, *J. Colloid Interface Sci.*, 2011, **361**, 205–211.
7 H. A. Al-Lohedan, *J. Chem. Soc., Perkin Trans. 2*, 1995, 1707–1713.
8 O. S. Tee, *Adv. Phys. Org. Chem.*, 1994, **29**, 1–85.
9 V. T. D'Souza and K. B. Lipkowitz, *Chem. Rev.*, 1998, **98**, 1741–1742.
10 K. A. Connors, *Chem. Rev.*, 1997, **97**, 1325–1357.
11 X. Zhang and C. Wang, *Chem. Soc. Rev.*, 2011, **40**, 94–101.
12 N. M. Rougier, D. L. Cruickshank, R. V. Vico, S. A. Bourne, M. R. Caira, E. I. Buján and R. H. de Rossi, *Carbohydr. Res.*, 2011, **346**, 322–327.
13 P. A. Prasantha, N. C. Sandhya, B. K. Kempegowda, D. G. Bhadregowda, K. Mantelingu, S. Ananda, K. K. S. Rangappa and M. N. Kumara, *J. Mol. Catal. A: Chem.*, 2012, **353–354**, 111–116.
14 D. J. Jobe, V. C. Reinsborough and S. C. Wetmore, *Langmuir*, 1995, **11**, 2476–2479.
15 H. Mwakibete, R. Cristantino, D. M. Bloor, W. Wyn-Jones and J. F. Holzwarth, *Langmuir*, 1995, **11**, 57–60.
16 A. J. M. Valente and O. Söderman, *Adv. Colloid Interface Sci.*, 2014, **205**, 156–176.
17 A. Raducan, A. Olteanu, M. Puiu and D. Oancea, *Cent. Eur. J. Chem.*, 2008, **6**, 89–92.

18 Y. Zhang, X. Li, J. Liu and X. Zeng, *J. Dispersion Sci. Technol.*, 2002, **23**, 473–481.
19 B. Samiey and A. R. Toosi, *Bull. Korean Chem. Soc.*, 2009, **30**, 2051–2056.
20 V. Raj, A. Sarathi, T. Chandrakala, S. Dhanalakshmi, R. Sudha and K. Rajasekaran, *J. Chem. Sci.*, 2009, **121**, 529–534.
21 O. Soriyan, O. Owoyomi and A. Ogunniyi, *Acta Chim. Slov.*, 2008, **55**, 613–616.
22 C. D. Ritchie, D. J. Wright, D. S. Huang and A. A. Kamego, *J. Am. Chem. Soc.*, 1975, **97**, 1163–1170.
23 F. J. Green, *The Sigma-Aldrich Handbook of Stains, Dyes and Indicators*, Aldrich Chemical Company, Inc., Milwaukee, Wisconsin, 1990.
24 W. Khon and L. J. Sham, *Phys. Rev.*, 1965, **140**, A1133.
25 G. M. Morris, R. Huey, W. Lindstrom, M. F. Sanner, R. K. Belew, D. S. Goodsell and A. J. Olson, *J. Comput. Chem.*, 2009, **30**, 2785–2791.
26 W. L. De Lano, *The PyMOL Molecular Graphics System*, De Lano Scientific, San Carlos, CA, USA, 2004.
27 Z. Yuanqin, Z. Xiancheng, Y. Xiaoqi and T. Anming, *J. Dispersion Sci. Technol.*, 1999, **20**, 437–448.
28 B. Dorrego, L. Garcia-Rio, P. Herves, J. R. Leis, J. C. Mejuto and J. Perez-Juste, *J. Phys. Chem. B*, 2001, **105**, 4912–4920.
29 Y. Moroi, *Micelles, Theoretical and Applied Aspects*, Plenum Press, New York, 1992, ch. 4.
30 S. Dasmandal, H. K. Mandal, A. Kundu and A. Mahapatra, *J. Mol. Liq.*, 2014, **193**, 123–131.
31 L. García-Río, J. R. Leis, J. C. Mejuto, A. Navarro-Vázquez, J. Pérez-Juste and P. Rodriguez-Dafonte, *Langmuir*, 2004, **20**, 606–613.
32 E. Rodenas and S. Vera, *J. Phys. Chem.*, 1985, **89**, 513–516.
33 C. A. Bunton, F. Nome, F. H. Quina and L. S. Romsted, *Acc. Chem. Res.*, 1991, **24**, 357–364.
34 C. A. Bunton, in *Surfactants in Solution*, ed. K. L. Mittal and D. O. Shah, Plenum Press, New York, 1991, vol. 11, p. 17.
35 C. A. Bunton and G. Savelly, *Adv. Phys. Org. Chem.*, 1986, **22**, 213–309.
36 F. F. Al-Blewi, H. A. Al-Loheadan, M. Z. A. Rafiquee and Z. A. Issa, *Int. J. Chem. Kinet.*, 2013, **45**, 1–9.
37 C. K. Ingold, *Structure and Mechanism in Organic Chemistry*, Bell, London, 1993.
38 R. L. VanEtten, J. F. Sevansian, G. A. Clowes and M. L. Bender, *J. Am. Chem. Soc.*, 1967, **89**, 3242–3253.
39 K. N. Raymond, C. J. Hastings, M. D. Pluth and R. G. Bergman, *J. Am. Chem. Soc.*, 2010, **132**, 6938–6940.
40 P. Beer, P. A. Gale and D. K. Smith, *Supramolecular Chemistry*, Oxford University Press, New York, 1999.
41 R. Breslow and S. D. Dong, *Chem. Rev.*, 1998, **98**, 1997–2011.
42 M. L. Benesi and J. H. Hildebrand, *J. Am. Chem. Soc.*, 1949, **71**, 2703–2707.
43 S. S. Mati, S. Sarkar, S. Rakshit, A. Sarkar and S. C. Bhattacharya, *RSC Adv.*, 2013, **3**, 8071–8082.
44 A. S. Balte, P. K. Goyal and S. P. Gejji, *J. Chem. Pharm. Res.*, 2012, **4**, 2391–2399.
45 Advanced Separation Technologies Inc., in *Cyclobond Handbook*, Printed in USA, 6th edn, 2002, p. 1.
46 T. Lengauer and M. Rarey, *Curr. Opin. Struct. Biol.*, 1996, **6**, 402–406.
47 A. M. Vijesh, A. M. Isloor, S. Telkar, T. Arulmoli and H. K. Fun, *Arabian J. Chem.*, 2013, **6**, 197–204.